

MMP13 as a stromal mediator in controlling persistent angiogenesis in skin carcinoma

Wiltrud Lederle^{1,2}, Bettina Hartenstein³, Alice Meides¹,
Heike Kunzelmann¹, Zena Werb⁴, Peter Angel³ and
Margareta M.Mueller^{1,*}

¹Group of Tumour and Microenvironment (A101), German Cancer Research Center (DKFZ), Im Neuenheimer Feld 280, 69120 Heidelberg, Germany,

²Department of Experimental Molecular Imaging Experimental Molecular Imaging, Medical Faculty, University of Aachen (RWTH), Pauwelsstrasse 20, 52074 Aachen, Germany, ³Division of Signal Transduction and Growth Control (A100), German Cancer Research Center (DKFZ), Im Neuenheimer Feld 280, 69120 Heidelberg, Germany and ⁴Department of Anatomy, University of California, San Francisco, CA 94143-0452, USA

*To whom correspondence should be addressed. Tel: +49 6221 42 4533;
Fax: +49 6221 42 4551;
Email: ma.mueller@dkfz-heidelberg.de

Matrix metalloproteinases (MMPs) such as MMP13 promote tumour growth and progression by mediating extracellular matrix (ECM) reorganization and regulating the biological activity of cytokines. Using *Mmp13*^{-/-} mice, we demonstrate an essential role of this single collagenase for highly malignant and invasive growth in skin squamous cell carcinoma (SCC). Lack of host MMP13 strongly impaired tumour growth of malignant SCC cells, leading to small, mostly avascular cysts. While initial stromal activation in tumour transplants of *Mmp13*^{+/+} and *Mmp13*^{-/-} animals was similar, MMP13 was essential for maintenance of angiogenesis and for invasion. MMP13 was induced in fibroblasts of the wild-type animals at the onset of invasion and correlated with a strong increase in vascular endothelial growth factor (VEGF) protein and its association with vascular endothelial growth factor receptor-2 on endothelial cells in invasive areas. In contrast, VEGF protein in the stroma was barely detectable and tumour invasion was downregulated in *Mmp13*^{-/-} animals, despite ongoing VEGF messenger RNA expression. Taken together with *in vitro* data showing the release of VEGF from the ECM by MMP13 expressing fibroblasts, these data strongly suggest a crucial role of MMP13 in promoting angiogenesis via releasing VEGF from the ECM and thus allowing the invasive growth of the SCC cells.

Introduction

Matrix metalloproteinases (MMPs), a family of structurally related zinc-dependent endopeptidases, are key regulators of tissue reorganization that occurs in wound healing, inflammatory responses and malignancy (1). In tumorigenesis, multiple and even opposite functions have been described for MMPs. They are involved in tumour initiation and progression, angiogenesis and activation of cytokines, but they can also exert tumour-inhibiting functions, e.g. by releasing anti-angiogenic factors (2,3). In the complex tumour tissue, MMPs expressed by both tumour and stromal cells cooperate to promote tumour initiation and progression. There are >20 different human MMPs (1,2). Among them, the collagenase subfamily, with the fibroblast interstitial collagenase (MMP1), the neutrophil collagenase (MMP8), collagenase-3 (MMP13) and MMP14, play important roles for tumour progression and invasion due to their ability to degrade fibrillar collagens and components of the basement membrane (1,4–9).

Abbreviations: cDNA, complementary DNA; ECM, extracellular matrix; mRNA, messenger RNA; MEF, mouse embryonic fibroblast; MMP, matrix metalloproteinase; mMMP13, mouse matrix metalloproteinase-13; s.c., subcutaneous; SCC, squamous cell carcinoma; SMA, smooth muscle actin; VEGF, vascular endothelial growth factor; VEGFR-2, vascular endothelial growth factor receptor-2.

Whereas MMP8 has pro-tumourigenic and protective functions (10), MMP1 and MMP13 are both associated with tumour growth and progression. Overexpression of human MMP1 has been demonstrated in a variety of advanced cancers like metastatic melanoma and colorectal, gastric, oesophageal, pancreatic and breast carcinoma (4,11–16). In breast cancer, MMP1 is associated with a poor clinical outcome (17) and is now discussed as a potential predictive marker even for precancerous lesions (18).

MMP13 is induced during invasion and metastasis of breast carcinomas, squamous cell carcinomas (SCCs), squamous cell carcinomas of the head and neck and melanomas (19–25). In breast cancer, MMP13 expression correlates with progression to invasive carcinomas (26). It is mainly attributed to stromal cells in close vicinity to tumour cells, supporting a crucial role of the stroma for tumour progression (24,27).

While these data clearly support the importance of MMP1 and MMP13 for the growth and progression of human cancer, the use of mouse models is indispensable to pinpoint their functional contribution. In mouse, the interstitial collagenase (MMP13) is homologous to human MMP13. However, the expression pattern of mouse MMP13 is comparable with human MMP1, strongly suggesting a functional homology between mouse MMP13 and both human MMP1 and MMP13 (5,19,28). Accordingly, mouse MMP13 plays a role in physiological and pathological tissue remodelling, e.g. during bone development and the early phase of wound healing (28–32). Mouse MMP13 is strongly upregulated in the stroma of breast cancer xenografts (33) and is induced in fibroblasts at the transition to invasion in a mouse mammary carcinoma model (34). We previously demonstrated a strong expression of MMP13 in the stroma of highly malignant HaCaT-ras skin SCC xenografts (35,36) and an almost complete downregulation in the non-invasive tumours that result from treatment with the angiogenesis inhibitor DC101 (35,37). This suggests a crucial function of MMP13 in driving tumour progression and invasive growth of skin SCCs.

In this study, we used *Mmp13*^{+/+} and *Mmp13*^{-/-} mice to analyze the functional role of MMP13 in growth, angiogenesis and invasion of early and advanced stages of skin carcinogenesis.

Material and methods

Transgenic animals

Mmp13^{-/-} mice were generated as described previously (32) and bred into a pure C57BL/6 background (>12 backcrosses). All animal experiments were performed in accordance with the governmental review committee on animal care (Regierungspräsidium Karlsruhe).

Cell lines

PDVA cells were generated by *in vitro* 7,12-dimethylbenz(a)anthracene treatment of B10LP mouse keratinocytes as described (38). BDVII cells were established from 7,12-dimethylbenz(a)anthracene-induced SCCs in C57BL/6 mice as described (39). PDVA and BDVII cells were cultured in Dulbecco's modified Eagle's medium with 10% fetal calf serum and tested negative for mycoplasma contamination as described (40). Mouse embryonic fibroblasts (MEFs) were isolated from *Mmp13*^{+/+} and *Mmp13*^{-/-} littermate embryos and immortalized as described (41).

Tumourigenicity assays *in vivo*: subcutaneous injection

A total of 5×10^6 BDVII cells were injected subcutaneously (s.c.) into both flanks of 5- to 6-week old *Mmp13*^{+/+} and *Mmp13*^{-/-} mice (four animals per group). Tumour size was measured weekly, and tumour volume was calculated as described (35). The injection was repeated three times.

Surface transplantation assay

Tumour cells (BDVII) precultured on a collagen type I gel were transplanted onto the dorsal muscle fascia of 5- to 6-week old *Mmp13*^{+/+} and *Mmp13*^{-/-} mice as described (42). For 5 weeks, four animals per group were killed and analyzed as described (35). The transplantation was repeated twice.

Transfilter cocultures

A total of 3×10^5 BDVII cells were cocultivated with 5×10^5 *Mmp13*^{+/+} and *Mmp13*^{-/-} MEFs in transfilter coculture chambers (3 µm phycoerythrin-filter Falcon, BD Biosciences, San Jose, CA). Coculture was initiated 1 day after cell seeding. RNA was isolated from the MEFs in the bottom wells using the RNeasy Mini Prep Kit (QIAGEN, Hilden, Germany). Each assay condition was tested in duplicate and repeated twice.

Tumorigenicity assay in vitro: organotypic cocultures

Dermal equivalents for organotypic cocultures containing 2.5×10^5 *Mmp13*^{+/+} or *Mmp13*^{-/-} MEFs were prepared with native type I rat collagen (final concentration of 3 mg/ml) as described (43). Tumour cells (8.5×10^5 PDVA cells) were seeded on top of the collagen matrix. For 3 weeks, two cultures per week were harvested and processed for cryostat sectioning. Data shown are representatives of two independent experiments.

VEGF release studies

Dermal equivalents with irradiated (30 Gy) non-proliferating *Mmp13*^{+/+} or *Mmp13*^{-/-} MEFs (5×10^5 cells/ml gel) were prepared as described (43) with 500 pg/ml, 2 ng/ml or 10 ng/ml recombinant human vascular endothelial growth factor (VEGF)-165 (R&D Systems, Wiesbaden, Germany) and cultured for 12 days. Conditioned medium was harvested every 72 h and VEGF concentrations were measured by enzyme-linked immunosorbent assay (human VEGF Quantikine ELISA Kit, R&D Systems). Each assay condition was tested in triplicate and repeated twice.

Reverse transcription-polymerase chain reaction analysis

Reverse transcription was performed with 0.5 µg messenger RNA (mRNA) (Omniscript Reverse Transcriptase; QIAGEN). Complementary DNA (cDNA) (diluted 1:10) was amplified with 0.2 mM deoxynucleotide triphosphates (Sigma-Aldrich, Taufkirchen, Germany), 5 U Taq polymerase (QIAGEN), 1.5 mM MgCl₂ and 0.15 µM of each primer at the annealing temperature indicated (mouse matrix metalloproteinase-13 (mMMP13) forward: 5'-CCTTCTGGTCTTCTGGCACAC-3' and mMMP13 reverse: 5'-GGCTGGGTCA-CACTTCTCTGG-3' (60°C); mouse β-tubulin forward: 5'-TCCTCTGTGCCTGAACCTACC-3' and mouse β-tubulin reverse: 5'-GGAACATAGCCGTAAACCTGC-3' (50°C) for 22–35 cycles. Polymerase chain reaction products were analyzed in 2% agarose gels (Biozym Diagnostic). Mouse β-tubulin was co-amplified with the target gene to confirm equal amounts of starting cDNA.

Real-time polymerase chain reaction

Reverse transcription was performed as described (QIAGEN). For quantification of relative mRNA levels, cDNAs were amplified and real-time fluorimetric intensity was monitored according to the manufacturer's instructions using universal probe library-based technology and the LightCycler® TaqMan® Master (Roche Diagnostics, Mannheim, Germany). The following primers were used: mMMP13 forward: 5'-cagctccgaggagaactatgat-3' and mMMP13 reverse: 5'-ggactttgcaaaaagactcag-3' and for mouse hypoxanthine phosphoribosyl transferase forward: 5'-tgatagatccattcctatgactgtaga-3' and mouse hypoxanthine phosphoribosyl transferase reverse: 5'-aagacattcttcagttaaagttgag-3'. The mouse hypoxanthine phosphoribosyl transferase signal was determined in duplicates for each cDNA and used for normalization. All primer sets were assayed for quantitative PCR effectiveness. Relative transcription levels were determined as described (44).

Antibodies

Primary antibodies were as follows: rat monoclonal antibody to mouse CD31 (BD PharMingen, Heidelberg, Germany), guinea pig pan-keratin anti-serum (Progen, Heidelberg, Germany), rabbit Ki-67 anti-serum (Acris, Bad Nauheim, Germany), rabbit collagen type IV anti-serum (Novotec, Lyon, France), biotinylated mouse monoclonal antibody to smooth muscle actin (SMA) (Progen), guinea-pig vimentin anti-serum (Progen), rat monoclonal antibody to mouse macrophages (ER-MP23; Acris), goat affinity purified antibody to murine MMP9 (R&D Systems), goat affinity purified antibody to murine VEGF (R&D Systems), goat affinity purified antibody to murine vascular endothelial growth factor receptor-2 (VEGFR-2) (R&D Systems). Sheep anti-MMP13 anti-serum (kind gift from G.Murphy, Cambridge, UK (45)). The specificity of the VEGF antibody was tested on HaCaT cells transfected with murine VEGF (data not shown). Secondary antibodies were obtained from Dianova, Hamburg, Germany.

Indirect immunofluorescence

Frozen sections were fixed in methanol and acetone and stained as described (43). Cell nuclei were counterstained with 20 µg/ml Hoechst 33258/bisbenzimidide (Sigma-Aldrich). Stained sections were examined with a Leica DM RBE fluorescence microscope (Leica GmbH, Wetzlar, Germany).

In situ hybridization

In situ hybridization was performed as described (35), using a digoxigenin-labelled probe for murine *VEGF-164* (kindly provided by G.Breier, Institute of Pathology Technische Universität Dresden, Germany). Digoxigenin signals were detected by anti-digoxigenin alkaline phosphatase (Roche Diagnostics, Mannheim, Germany) and NBT-BCIP substrate reaction (Promega, Mannheim, Germany). Sections were counterstained against pan-keratin and collagen type IV and examined as described above. For better visualization of digoxigenin signals, colours were reassigned with the analySIS software (Soft Imaging Systems, Münster, Germany).

In situ zymography

Proteolytic activity against collagen IV was demonstrated in unfixed cryostat sections using DQ collagen IV D-12052 (EnzChek; Molecular Probes, Invitrogen, Karlsruhe, Germany) as a substrate. Cryostat sections (7 µm) were incubated with 40 µg/ml DQ collagen IV in 1× reaction buffer (0.5 M Tris-HCl, 1.5 M NaCl, 50 mM CaCl₂, 2 mM sodium azide, pH 7.6) and counterstained by Hoechst 33258/bisbenzimidide for 2 h at room temperature. After washing (3 × 5 min in phosphate-buffered saline), sections were fixed in methanol and acetone and photographed with a Leica DM RBE fluorescence microscope (Leica GmbH).

Morphometric analysis

Quantification was performed for three areas of 1.5 mm² per section of four different animals from two independent transplantation series, using the analySIS software.

Statistics

Two-tailed Student's *t*-test was used for data analysis, with **P* < 0.05 considered as statistically significant and ***P* < 0.001 as highly significant.

Results*Stromal MMP13 is crucial for invasive growth of SCC cells*

The role of stromal MMP13 in tumour growth of skin SCC was determined by s.c. injecting syngeneic BDVII SCC tumour cells (39) into *Mmp13*^{+/+} and *Mmp13*^{-/-} mice. In three independent experiments, BDVII SCC cells formed fast growing tumours in *Mmp13*^{+/+} mice, reaching a mean size of ~1.8 cm³ after 4 weeks. In contrast, lack of MMP13 in *Mmp13*^{-/-} mice restricted tumour growth to small nodules reaching sizes of only 0.13 cm³ after 4 weeks (Figure 1A).

To further determine the reasons for this difference in tumour growth, tumour sections were analyzed by immunohistology. Hoechst staining of cell nuclei combined with vascular endothelial cell staining by CD31 and keratin staining of the complete tumour mass demonstrated that tumour vascularization and invasion into the host stroma were dramatically impaired by the lack of stromal MMP13. In contrast to the well vascularized and highly invasive tumours of the *Mmp13*^{+/+} mice, tumour nodules of *Mmp13*^{-/-} animals consisted mostly of terminally differentiated cornified tissue with a small rim of vital tumour cells that was only marginally infiltrated by blood vessels (Figure 1B). Vital tumour cells were characterized by their double-positive staining for Hoechst (blue) and keratin (green), whereas no Hoechst stained nuclei were detected in the keratin-positive cornified areas consisting of terminally differentiated epithelial cells (Figure 1B). Analysis of cell proliferation by Ki67 staining confirmed that cell proliferation was restricted to the vital tumour cells containing Hoechst-positive nuclei and was absent in the strongly keratinized regions that lacked nuclear staining (Figure 1C). However, the proliferation rate in the vital tumour area was comparable between *Mmp13*^{+/+} and *Mmp13*^{-/-} mice (Figure 1C).

MMP13 is expressed in vascularized tumour areas and localized to fibroblasts

The differences in tumour vascularization indicated the involvement of stromal MMP13 in angiogenesis. We therefore analyzed the localization of MMP13 in the tumour stroma. In *Mmp13*^{+/+} (Figure 2A), but not in *Mmp13*^{-/-} mice (Figure 2B), MMP13 protein was detected in the tumour invading stromal strands in close proximity to

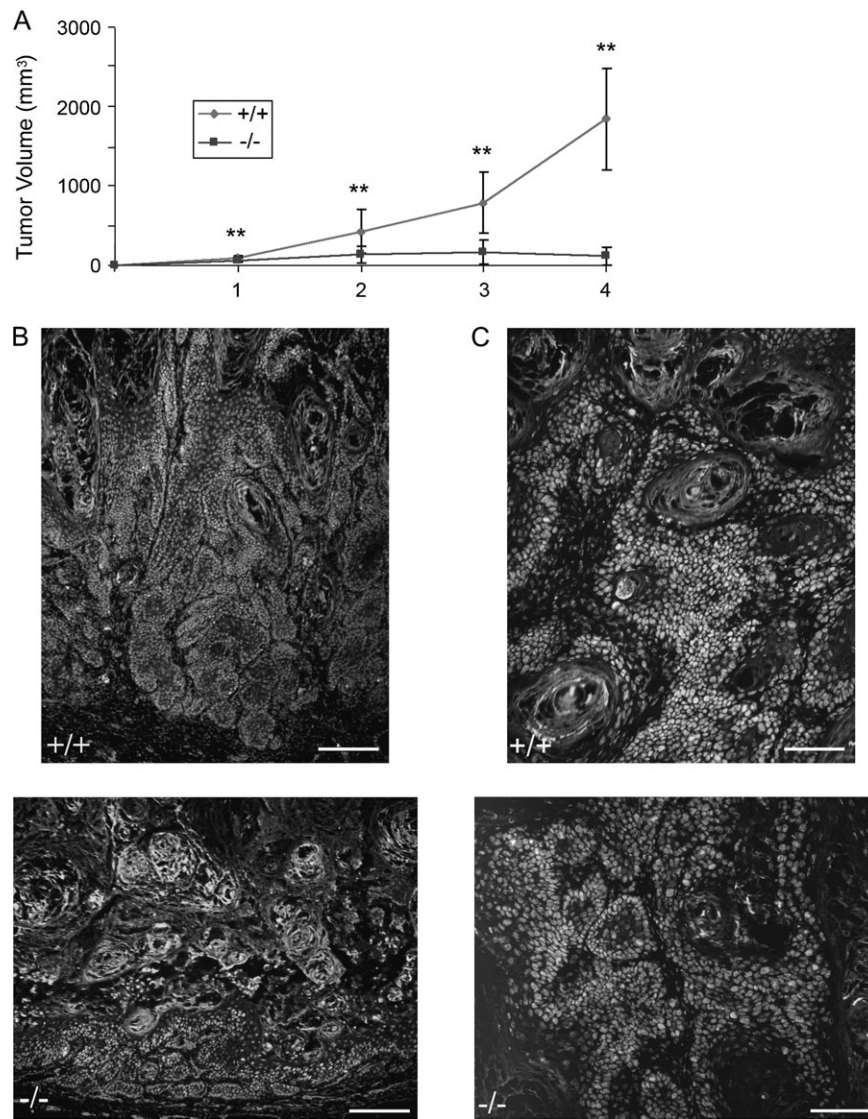


Fig. 1. Stromal MMP13 drives tumour growth and invasiveness in skin SCC. (A) Tumour growth curves of BDVII SCC cells upon s.c. injection into *Mmp13*^{+/+} and *Mmp13*^{-/-} mice, $**P < 0.001$. (B) Immunostaining of blood vessels against CD31 (red), tumour tissue against pan-keratin (green) and nuclei by Hoechst (blue), bar 200 μ m. (C) Analysis of cell proliferation by immunostaining of Ki67 (red), keratinized tumor areas (keratin, green) and nuclei (Hoechst, blue), bar 100 μ m.

CD31-positive blood vessels. MMP13 protein did not directly colocalize with the endothelial cells (Figure 2A), and staining of tissue macrophages (ER-MP23 antibody) additionally excluded its colocalization with macrophages that were located at the outer stromal rim of the tumours far away from the vascularized MMP13-positive invasive areas (Figure 2C). In contrast, costaining of MMP13 with the myofibroblast marker SMA (Figure 2D, counterstaining CD31) or the fibroblast marker vimentin (Figure 2E, counterstaining keratin) revealed a close colocalization with the signals for MMP13. This suggested fibroblasts or myofibroblasts as main MMP13 producers and is in agreement with the previously described MMP13 expression in myofibroblasts at the tumour stroma border in the polyomavirus middle T breast carcinoma model (34).

MMP13 expressed by fibroblasts supports the invasive growth of SCC cells in vitro

To further confirm the MMP13 expression by fibroblasts and to analyze the impact of the SCC cells on the expression level, fibroblasts isolated from *Mmp13*^{+/+} and *Mmp13*^{-/-} littermate embryos were cultivated in transfilter cocultures in the absence or presence of BDVII

SCC cells and *Mmp13* mRNA expression was determined by semi-quantitative reverse transcription-polymerase chain reaction (A) and by real-time polymerase chain reaction (B). *Mmp13*^{+/+} MEFs expressed *Mmp13* already in the absence of SCC cells (Figure 3A, panel 1 and Figure 3B, bar 1) yet, the expression was markedly upregulated in the presence of BDVII cells (Figure 3A, panel 3 and Figure 3B, bar 3).

In order to determine the direct influence of MMP13 expressing fibroblasts on growth and invasion of skin SCCs on collagen I, the substrate for MMP13, we established 3D organotypic cocultures of *Mmp13*^{+/+} or *Mmp13*^{-/-} MEFs with PDVA SCC cells. In contrast to the C57BL/6-derived BDVII SCC cells that were used for *in vivo* experiments and show a very extensive differentiation under *in vitro* growth conditions (data not shown), PDVA cells (derived from B10LP mice) proliferate well and form a multilayered three-dimensional epithelium with invasive capacities under these *in vitro* culture conditions. Haematoxylin and eosin staining demonstrated the presence of invasive tumour islets in the collagen gel (Figure 3C, arrows) in 3-week-old cocultures with *Mmp13*^{+/+} MEFs, associated with a reduced and interrupted collagen IV staining (Figure 3D, arrows).

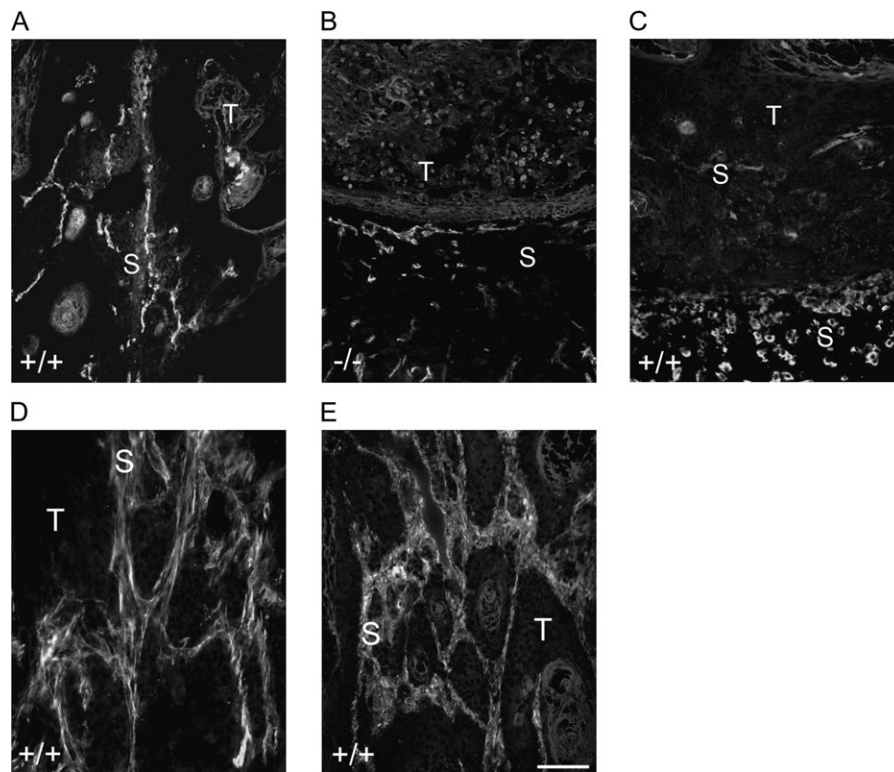


Fig. 2. MMP13 is expressed in the invasive areas close to blood vessels and associated with fibroblasts. (A and B) Immunostaining of MMP13 (red) in the s.c. tumours of *Mmp13*^{+/+} (A) and *Mmp13*^{-/-} (B) animals, counterstaining of CD31-positive blood vessels (green) and of the tumour tissue against pan-keratin (blue). (C) Immunostaining for MMP13 (red), ER-MP23-positive macrophages (green) and pan-keratin (blue) of s.c. tumours from *Mmp13*^{+/+} animals. (D and E) Immunostaining for MMP13 (red, D and E) and smooth muscle actin (green, D), CD31 (blue, D) or vimentin (green, E) and pan-keratin (blue, E) of s.c. tumours from *Mmp13*^{+/+} animals. Bar 100 μ m (A–E), T, tumour; S, stroma.

In contrast, cocultures with *Mmp13*^{-/-} MEFs showed a continuous collagen IV staining at the basement membrane zone and a more regular epithelial border (Figure 3C and D). However, proliferation rate of the PDVA cells was comparable in cocultures with *Mmp13*^{+/+} and *Mmp13*^{-/-} MEFs, as demonstrated by Ki67 staining (Figure 3E). In addition, a strong proteolytic activity against collagen IV was detected in the basement membrane zone of cocultures with *Mmp13*^{+/+} fibroblasts (Figure 3F–H, left panels, arrows mark the areas with proteolytic activity), whereas no proteolytic activity against collagen IV was detected in the basement membrane zone of cocultures with *Mmp13*^{-/-} MEFs (Figure 3F–H, right panels, arrowheads show the lack of collagenolytic activity). These data support a role of fibroblast-derived MMP13 for the invasive growth of malignant SCC cells.

Lack of stromal MMP13 strongly impairs tumour vascularization

The only moderate invasive growth behaviour of the SCC cells in the organotypic cocultures suggested a more complex function of MMP13 beyond simple collagen degradation. To determine the specific contribution of MMP13 to initial tumour growth, angiogenesis and invasion in the complex tissue environment *in vivo*, BDVII SCC cells were transplanted as preformed epithelia on collagen type I gels onto the muscle fascia of *Mmp13*^{+/+} and *Mmp13*^{-/-} mice. In this model, the collagen gel delays the contact between tumour and stroma but allows the interaction via diffusible factors, thereby enabling the detailed characterization and temporal analysis of stromal activation, cellular recruitment, angiogenesis and invasion (42).

The recruitment of SMA-positive fibroblasts was similar in transplants of *Mmp13*^{+/+} and *Mmp13*^{-/-} animals during the whole observation period (data not shown). In contrast, the angiogenic response and initial tumour cell infiltration into the stroma were only comparable between early transplants of *Mmp13*^{+/+}

and *Mmp13*^{-/-} mice, as analyzed by immunostaining to CD31 (endothelial cells), pan-keratin (tumour tissue) and Hoechst (nuclei of vital tumour cells). Significant differences became obvious starting from week 3 post-transplantation. In transplants of *Mmp13*^{+/+} animals, angiogenesis and tumour cell invasion were maintained, resulting in large invasive and highly vascularized tumours at week 4–5 (Figure 4A). In contrast, vascularization of the tumour tissue was dramatically impaired in the absence of host MMP13, leading to a mostly avascular cornified tumour tissue at week 4–5 and to an almost complete abrogation of tumour cell invasion (Figure 4A). Quantification confirmed an equal vessel density in the invasive areas 2 weeks post-transplantation (Figure 4B) but a significantly reduced vascular density in the tumour tissue starting from week 3 in transplants of *Mmp13*^{-/-} animals compared with transplants of *Mmp13*^{+/+} mice (Figure 4B). These data suggest a crucial contribution of MMP13 to the maintenance of angiogenesis and tumour invasion.

MMP13 induction is associated with a strong VEGF protein increase in the angiogenic areas

To further pinpoint the role of MMP13 in angiogenesis and invasion, we analyzed the kinetics of MMP13 expression in the surface transplants of wild-type animals by immunostaining with antibodies to MMP13, CD31 (vascular endothelial cells) and pan-keratin (tumour tissue). While MMP13 protein was absent in transplants of wild-type animals 2 weeks post-transplantation (Figure 5A), it appeared at week 3 and was strongly detected in the stromal strands at week 4 and 5 after transplantation concomitantly with the establishment of a highly vascularized and invasive tumour phenotype (Figure 5A). In addition, MMP13 expression coincided with a strong increase in VEGF protein in the invasive areas around blood vessels starting from week 3 (Figure 5B), whereas VEGF was only very weakly detected at the

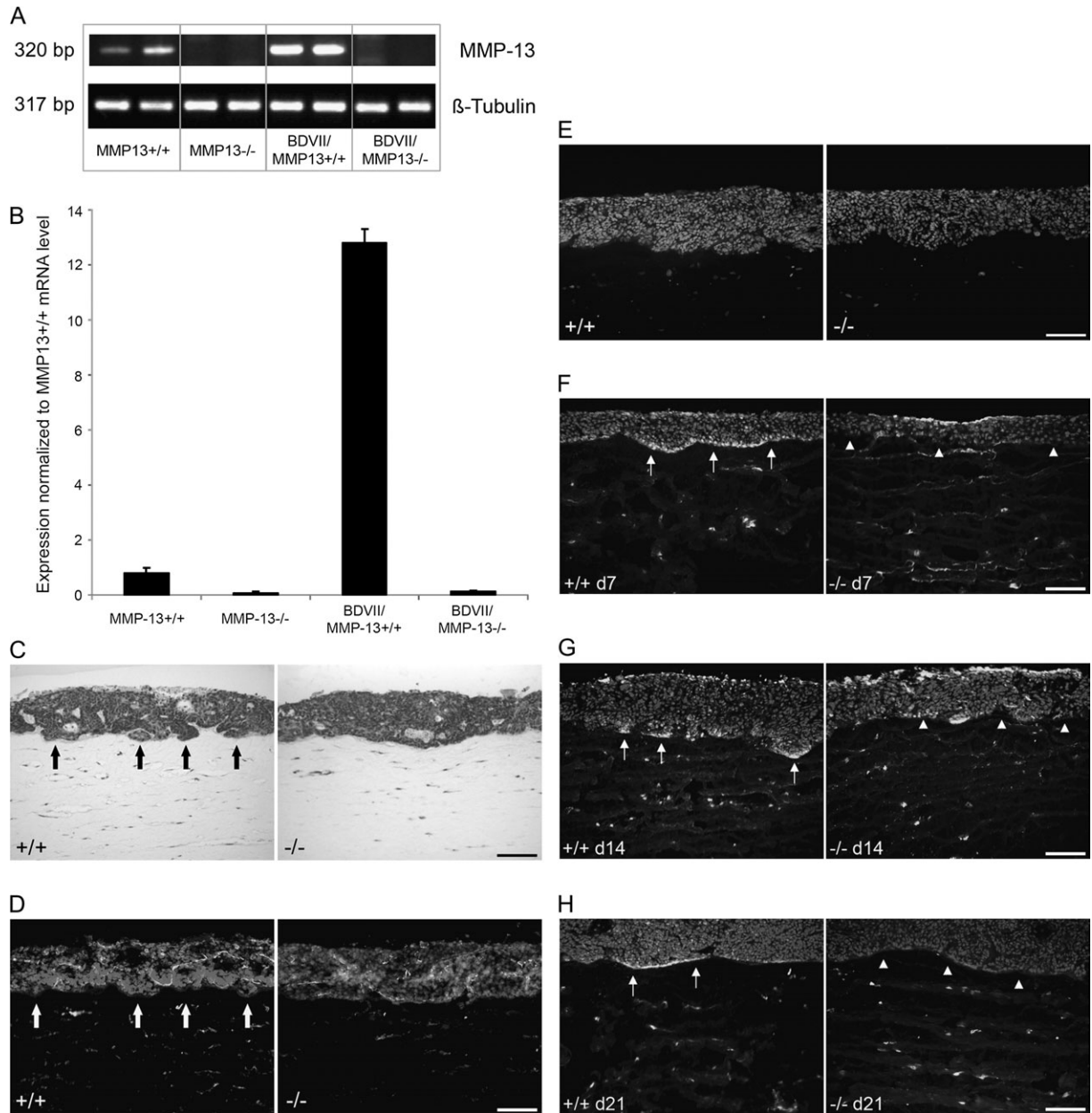


Fig. 3. MMP13 expressing fibroblasts promote the invasive growth in organotypic cocultures. (A) Reverse transcription–polymerase chain reaction analysis of MMP13 in MEFs isolated from *Mmp13*^{+/+} and *Mmp13*^{-/-} in the absence (panels 1 and 2) and presence of BDVII cells (panels 3 and 4) of two cultures each. (B) Real-time polymerase chain reaction analysis of MMP13 expression in *Mmp13*^{+/+} (bars 1 and 3) and *Mmp13*^{-/-} MEFs (bars 2 and 4) alone (bars 1 and 2) and in coculture with BDVII cells (bars 3 and 4). (C) Haematoxylin and eosin staining of 3-week-old organotypic cocultures of PDVA SCC cells with *Mmp13*^{+/+} and *Mmp13*^{-/-} MEFs. Arrows mark the invasive areas in the cultures containing *Mmp13*^{+/+} MEFs. (D) Immunostaining against collagen IV (green) of 3-week-old organotypic cocultures of PDVA cells with *Mmp13*^{+/+} and *Mmp13*^{-/-} MEFs, nuclei stained by Hoechst (blue). Arrows mark the interrupted collagen IV staining in the cultures containing *Mmp13*^{+/+} MEFs. (E) Immunostaining against the proliferation associated antigen Ki67 (red) in 3-week-old cocultures of PDVA cells with *Mmp13*^{+/+} and *Mmp13*^{-/-} MEFs, nuclei stained by Hoechst (blue). (F–H) *In situ* zymography for proteolytic activity against collagen IV in organotypic cocultures after 7, 14 and 21 days of culture with *Mmp13*^{+/+} MEFs (left panels, arrows mark the areas with collagenolytic activity) and in organotypic cocultures with *Mmp13*^{-/-} MEFs (right panels, arrowheads show respective areas without collagenolytic activity), nuclei are counterstained by Hoechst (blue); Bars 100 μm (C–H).

tumour stroma border in 4- and 5-week-old transplants of *Mmp13*^{-/-} animals (Figure 5B). Additionally, immunostaining of VEGF (Figure 6A, panels 1 and 3) and VEGFR-2 (Figure 6A, panels 2 and 4) on parallel cryosections of s.c. tumours revealed that VEGF colocalized with the VEGFR-2 on activated endothelial cells, suggesting the presence of receptor-bound VEGF (Figure 6A, panels 1 and 2). In tumours of *Mmp13*^{-/-} mice, the almost complete lack of VEGF protein staining coincided with a strong decrease in VEGFR-2 staining (Figure 6A, panels 3 and 4).

Despite this striking difference in detectable VEGF protein, we found no difference in *VEGF* mRNA expression, as determined by *in situ* hybridization with a probe specific for murine *VEGF-164* (Figure 6B and C). *VEGF* mRNA was strongly expressed by tumour and stromal cells in surface transplants of both, *Mmp13*^{+/+} and *Mmp13*^{-/-} animals at early and late time points.

One possible explanation for this discrepancy in mRNA detection and protein staining might be sequestration of VEGF protein in the extracellular matrix (ECM) in the absence of MMP13, thus

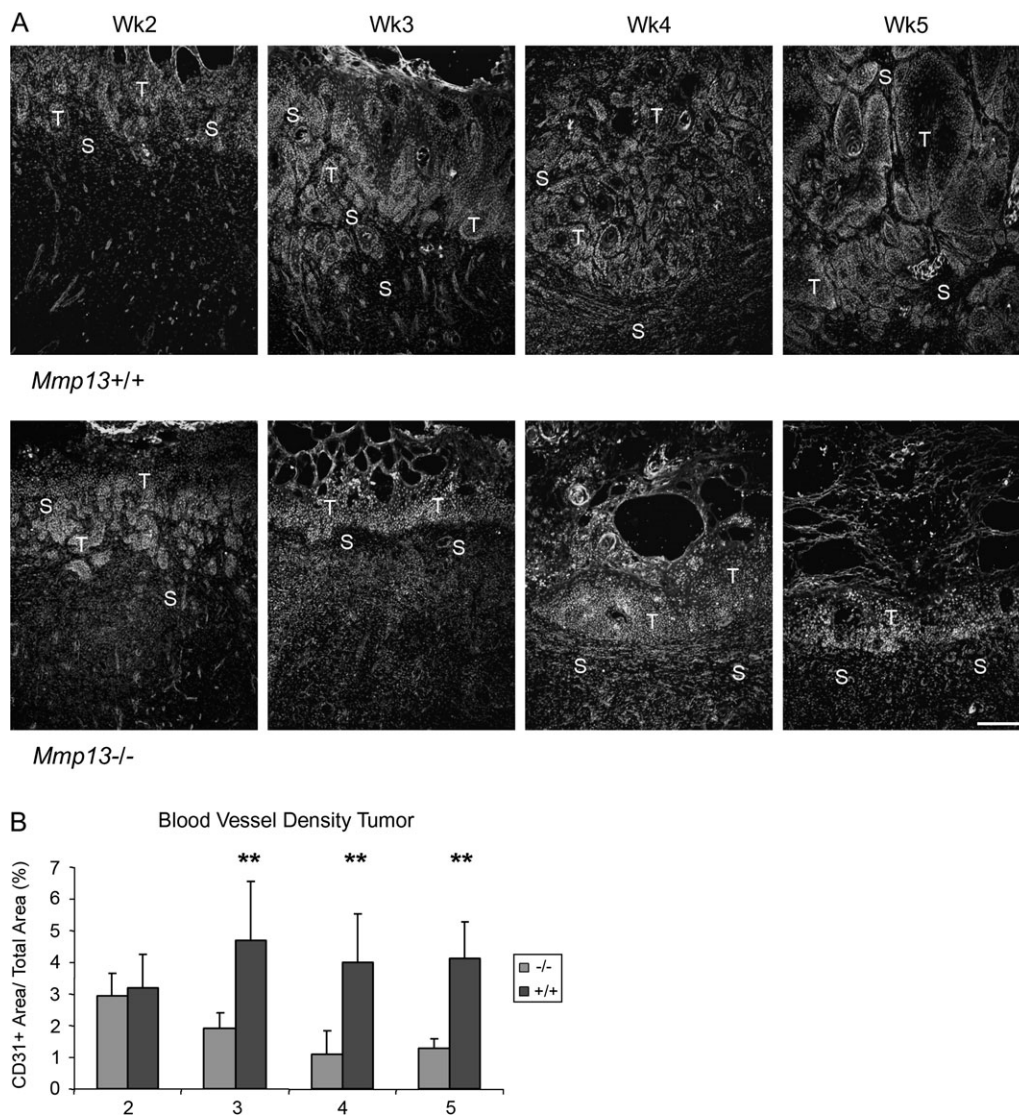


Fig. 4. Kinetics of angiogenesis and tumour growth in surface transplants. **(A)** Analysis of angiogenesis and tumour invasion in surface transplants of *Mmp13*^{+/+} and *Mmp13*^{-/-} mice. Immunostaining of CD31-positive endothelial cells (red) and pan-keratin-positive tumour tissue (green), nuclei stained by Hoechst (blue), bar 200 μ m; T, tumour; S, stroma. **(B)** Quantification of vessel density in the tumour tissue of surface transplants of *Mmp13*^{+/+} and *Mmp13*^{-/-} animals, bars: means \pm SDs of two transplantation series, four animals each, $**P < 0.001$.

preventing sufficient antibody binding for detection. To determine this, we generated dermal equivalents consisting of *Mmp*^{+/+} and *Mmp13*^{-/-} MEFs embedded in a collagen type I gel that contained different concentrations of human VEGF-165 (0.5–10 ng/ml). The amount of human VEGF released was measured by a species-specific enzyme-linked immunosorbent assay in conditioned media over a period of 12 days. The retention of VEGF in the gel was clearly enhanced in gels containing fibroblasts as compared to gels without fibroblasts (data not shown), suggesting the presence of additional ECM components that had been produced by fibroblasts and were able to bind VEGF. Independently of the initial concentration in the gel, VEGF concentrations released into the conditioned media of gels containing *Mmp13*^{+/+} MEFs were higher than for gels with *Mmp13*^{-/-} MEFs (Figure 6D, representative data shown for 500 pg/ml at day 6). This also held true for gels containing the fibroblasts in a fibronectin- and heparin-enriched collagen gel (data not shown). These results strongly indicate that MMP13 mediates the release of VEGF from dermal equivalents with wild-type fibroblasts.

Discussion

Our study demonstrates a crucial contribution of MMP13 to tumour progression of skin SCCs by maintaining angiogenesis and tumour cell invasion and thus augments the recently discovered novel roles of MMPs in tumourigenesis. Besides directly facilitating tumour cell migration and invasion through ECM degradation, MMPs have been demonstrated to exert indirect pro-tumourigenic functions by releasing growth factors from the ECM (1,46). Among them are the transforming growth factor beta or the basic fibroblast growth factor with a relatively broad range of action. Additionally, recent studies have demonstrated a critical role for MMP9 in mediating the release of the key angiogenic factor VEGF from the ECM, thereby stimulating angiogenesis and the initial onset of tumour growth (47). Using *Mmp13*^{+/+} and *Mmp13*^{-/-} mice, we now demonstrate a similar crucial function for MMP13 in driving tumour vascularization and invasion by promoting the persistent release of VEGF from the ECM at sites of invasion. While the s.c. injection of SCC cells in *Mmp13*^{+/+} mice induced the formation of highly vascularized invasive tumours, the tumours formed in *Mmp13*^{-/-} mice were small and

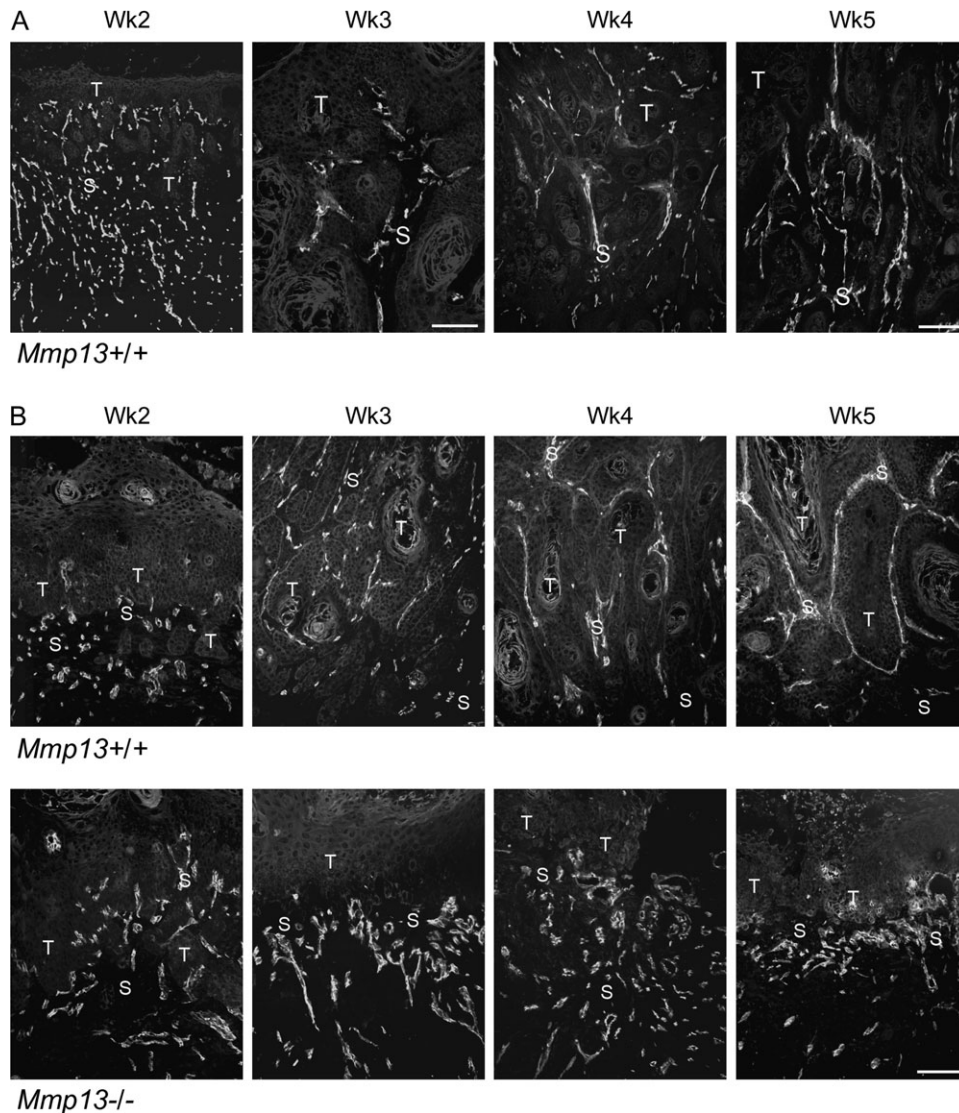


Fig. 5. Kinetics of MMP13 and VEGF protein expression in surface transplants. (**A** and **B**) Immunofluorescent staining against MMP13 (red, **A**), VEGF (red, **B**), CD31 (green) and pan-keratin (blue) of cryosections from surface transplants of *Mmp13*^{+/+} and *Mmp13*^{-/-} animals, bar 200 μ m in **A** (2nd panel 100 μ m), 100 μ m in **B**; T, tumour; S, stroma.

barely vascularized cornified cysts. Similar results have been recently demonstrated for melanoma, where host MMP13 plays a crucial role in promoting tumour vascularization and invasion (48). However, in contrast to the endothelial MMP13 expression observed in melanoma, MMP13 did clearly not colocalize with endothelial cells in tumours of wild-type mice in our skin SCC-model, although it was detected in the invasive areas nearby blood vessels. Colocalization studies for macrophages that were identified as MMP13 producers in the chorioallantoic membrane assay and in fibrotic lung tissue (49,50) also excluded macrophages as cellular source of host MMP13, since they were located at the outer stromal rim far away from the invasive areas. In contrast, MMP13 protein was found in close vicinity to SMA-positive cells and partially colocalized with vimentin-positive cells, strongly suggesting stromal fibroblasts as the main source of MMP13. Expression of MMP13 was described previously for skin fibroblasts (51) and breast cancer cell-associated myofibroblasts (34). The hypothesis of stromal fibroblasts as source of MMP13 was substantiated by *in vitro* experiments, showing basal MMP13 expression in fibroblasts isolated from *Mmp13*^{+/+} embryos that was strongly upregulated in coculture with SCC cells. More importantly, in three-dimensional organotypic cocultures *Mmp13*^{+/+} fibroblasts but not *Mmp13*^{-/-} fibroblasts

supported the invasive growth of SCC cells into the collagen gel and the degradation of the basement membrane component collagen IV. Although MMP13 is mostly described as protease targeting interstitial collagens, it has been demonstrated to effectively cleave also collagen IV (52). In agreement with this, we detected a strong proteolytic activity against collagen IV in the basement membrane zone of organotypic cocultures with *Mmp13*^{+/+} fibroblasts, whereas no activity was observed in cocultures with *Mmp13*^{-/-} fibroblasts. However, the only moderately invasive growth behaviour of the SCC cells in the 3D organotypic cocultures compared to the s.c. tumours suggested that MMP13 exerts additional invasion supporting functions beyond simply degrading interstitial collagens and collagen IV.

This became obvious by analyzing tumour growth, invasion and angiogenesis in the surface transplantation model, where the tumour cells are initially separated from the host tissue by a collagen type I gel. While MMP13 was clearly needed for the establishment of an invasive tumour phenotype, kinetic analyses revealed that host MMP13 was not responsible for initial tumour growth and the early stromal activation. During the first 2 weeks after transplantation, MMP13 expression was absent and initial angiogenesis and tumour cell invasion into the stromal compartment were comparable in

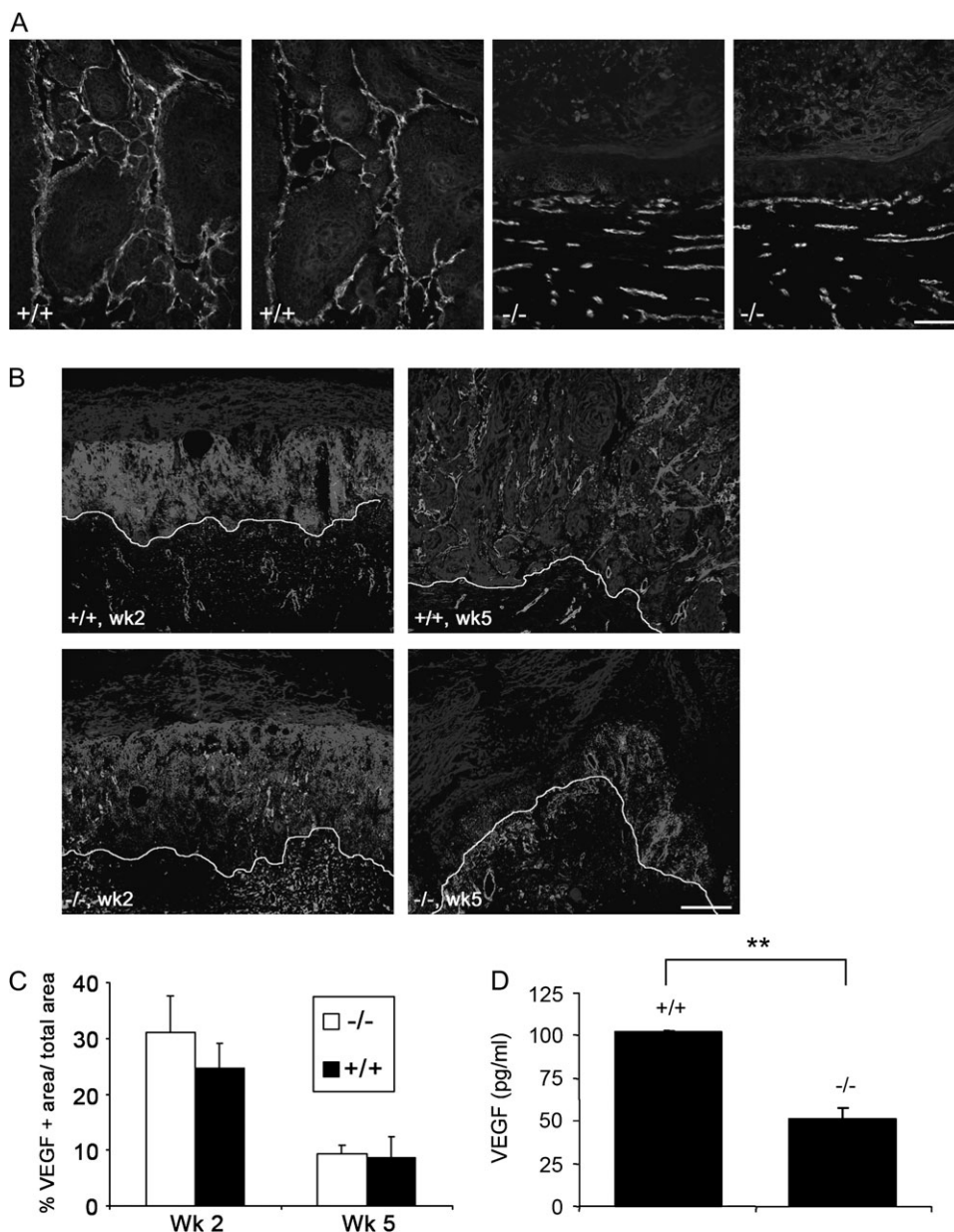


Fig. 6. MMP13 mediates the release of VEGF from the ECM. (A) Immunostaining on parallel cryosections of s.c. tumours from *Mmp13*^{+/+} (panels 1 and 2) and *Mmp13*^{-/-} mice (panels 3 and 4) for VEGF (red, panels 1 and 3), VEGFR-2 (red; panels 2 and 4), CD31 (green) and pan-keratin (blue), bar 100 µm. (B) Non-radioactive *in situ* hybridization with a murine *VEGF-164* probe (red) of early (left panels) and late (right panels) surface transplants of *Mmp13*^{+/+} (upper panels) and *Mmp13*^{-/-} (lower panels) mice, with immunofluorescent staining of blood vessels against collagen IV (green) and tumour tissue against pan-keratin (blue), bar 200 µm. The line marks the tumour stroma border. (C) Quantification of VEGF expression in surface transplants of *Mmp13*^{+/+} and *Mmp13*^{-/-} mice (VEGF-positive area/total area). (D) Release of human VEGF-165 from a collagen type I gel containing *Mmp13*^{+/+} or *Mmp13*^{-/-} MEFs, VEGF levels were measured by enzyme-linked immunosorbent assay, data shown for conditioned media of day 6 with 500 pg/ml of VEGF in the gel, ***P* < 0.001.

Mmp13^{+/+} and *Mmp13*^{-/-} animals. MMP13 expression was induced in the wild-type mice at week 3 after transplantation coinciding with the maintenance of angiogenesis and expression of the interstitial collagenase resulted in highly invasive and vascularized tumour transplants comparable with the s.c. tumours. In contrast, angiogenesis and tumour invasion were reduced in the absence of host MMP13, leading to a mostly avascular cornified tumour tissue like in the s.c. tumours. These observations strongly suggested a crucial role of MMP13 in the maintenance of angiogenesis at the invasive tumour stage. In support of this hypothesis, MMP13 induction in wild-type animals coincided with a strong increase in VEGF protein staining within these invasive areas, whereas VEGF protein was only weakly detected at the tumour stroma border in the knockout transplants. In addition, immunostain-

ing on parallel cryosections from s.c. tumours of wild-type animals demonstrated that VEGF protein was strongly enriched around blood vessels and colocalized with the VEGFR-2, indicating the presence of active VEGF bound to its receptor. In contrast, VEGF protein was almost absent and staining for VEGFR-2 was strongly decreased in tumours of *Mmp13*^{-/-} mice. These observations suggested that MMP13 is involved in ongoing angiogenesis via VEGF-mediated effects. However, the differences in protein staining were not based on different *VEGF* expression levels, since we detected a strong expression of *VEGF* mRNA in tumour and stromal cells of both, *Mmp13*^{+/+} and *Mmp13*^{-/-} animals. The drastic reduction in VEGF protein staining despite ongoing mRNA expression in *Mmp13*^{-/-} animals could be due to sequestration of VEGF in the absence of host

MMP13, thus preventing sufficient antibody binding for detection. In *Mmp13*^{+/+} animals, MMP13 might release VEGF from the ECM, thereby allowing its binding to the VEGFR-2 on endothelial cells and thus promoting angiogenesis, as it was described for MMP9 in early tumorigenesis of the Rip1Tag2 model (47). This hypothesis was substantiated *in vitro* by generating dermal equivalents of *Mmp13*^{+/+} or *Mmp13*^{-/-} fibroblasts embedded in a collagen type I gel containing human VEGF. The amount of VEGF that was released to the medium was clearly enhanced in the dermal equivalents with *Mmp13*^{+/+} fibroblasts. Thus, we postulate that MMP13 promotes the maintenance of angiogenesis in wild-type animals by releasing ECM-bound VEGF. While lack of MMP13 did not affect angiogenesis and tumour growth in a polyoma middle T antigen mammary carcinoma model possibly due to the compensatory effects of other proteolytic enzymes (34), angiogenesis promoting functions of MMP13 were described previously in the CAM assay (50). Indirect evidence for VEGF and angiogenesis regulating functions of MMP13 also comes from detailed analyses of *Mmp13*^{-/-} embryos which showed delayed endochondral ossification and a reduced vascularization of the primary ossification center at day 15.5 (29). Again, VEGF mRNA expression in the ossification centre was abundant, suggesting the reduced availability of VEGF protein as potential reason for this phenotype. In further agreement with a VEGF-mediated role of MMP13 in angiogenesis, *JunB*-deficient endothelial cells that show strongly decreased levels of endogenous MMP13 failed to form capillary-like networks in matrigel (53). The detailed mechanism by which MMP13 releases VEGF from the ECM, e.g. by degradation of VEGF-binding fibronectin is subject of further investigation (52,54).

In summary, our data strongly suggest a novel role of MMP13 in promoting tumour malignancy and invasion by maintaining and enhancing angiogenesis through the release of VEGF from the tumour ECM. Our studies clearly strengthen the crucial contribution of the tumour microenvironment to the growth of malignant cells and emphasize the importance of analyzing the role of specific MMPs in tumour initiation and progression to identify potentially successful therapeutic targets.

Funding

European Union FP6 Cancer Degradome, Deutsche Forschungsgemeinschaft (SPP1190 project Mu1830/3-1, SFB TR23); National Cancer Institute, USA (CA105379, CA072006).

Acknowledgements

The authors thank H.Steinbauer, R.Beck, K.Knebel, S.Teurich and B.Dittrich for providing reagents and excellent technical assistance.

Conflict of Interest Statement: None declared.

References

- Egeblad,M. *et al.* (2002) New functions for the matrix metalloproteinases in cancer progression. *Nat. Rev. Cancer*, **2**, 161–174.
- Lynch,C.C. *et al.* (2002) Matrix metalloproteinases in tumor-host cell communication. *Differentiation*, **70**, 561–573.
- Martin,M.D. *et al.* (2007) The other side of MMPs: protective roles in tumor progression. *Cancer Metastasis Rev.*, **26**, 717–724.
- Ala-aho,R. *et al.* (2005) Collagenases in cancer. *Biochimie*, **87**, 273–286.
- Balbin,M. *et al.* (2001) Identification and enzymatic characterization of two diverging murine counterparts of human interstitial collagenase (MMP-1) expressed at sites of embryo implantation. *J. Biol. Chem.*, **276**, 10253–10262.
- Sternlicht,M.D. *et al.* (2001) How matrix metalloproteinases regulate cell behavior. *Annu. Rev. Cell Dev. Biol.*, **17**, 463–516.
- Stamenkovic,I. (2000) Matrix metalloproteinases in tumor invasion and metastasis. *Semin. Cancer Biol.*, **10**, 415–433.
- Brinckerhoff,C.E. *et al.* (2000) Interstitial collagenases as markers of tumor progression. *Clin. Cancer Res.*, **6**, 4823–4830.
- Vihinen,P. *et al.* (2002) Matrix metalloproteinases in cancer: prognostic markers and therapeutic targets. *Int. J. Cancer*, **99**, 157–166.
- Van Lint,P. *et al.* (2006) Matrix metalloproteinase-8: cleavage can be decisive. *Cytokine Growth Factor Rev.*, **17**, 217–223.
- Murray,G.I. *et al.* (1996) Matrix metalloproteinase-1 is associated with poor prognosis in colorectal cancer. *Nat. Med.*, **2**, 461–462.
- Murray,G.I. *et al.* (1998) Matrix metalloproteinases and their inhibitors in gastric cancer. *Gut*, **43**, 791–797.
- Murray,G.I. *et al.* (1998) Matrix metalloproteinase-1 is associated with poor prognosis in oesophageal cancer. *J. Pathol.*, **185**, 256–261.
- Ito,T. *et al.* (1999) Expression of the MMP-1 in human pancreatic carcinoma: relationship with prognostic factor. *Mod. Pathol.*, **12**, 669–674.
- Nikkola,J. *et al.* (2005) High serum levels of matrix metalloproteinase-9 and matrix metalloproteinase-1 are associated with rapid progression in patients with metastatic melanoma. *Clin. Cancer Res.*, **11**, 5158–5166.
- Minn,A.J. *et al.* (2005) Genes that mediate breast cancer metastasis to lung. *Nature*, **436**, 518–524.
- van 't Veer,L.J. *et al.* (2002) Gene expression profiling predicts clinical outcome of breast cancer. *Nature*, **415**, 530–536.
- Poola,I. *et al.* (2005) Identification of MMP-1 as a putative breast cancer predictive marker by global gene expression analysis. *Nat. Med.*, **11**, 481–483.
- Freije,J.M. *et al.* (1994) Molecular cloning and expression of collagenase-3, a novel human matrix metalloproteinase produced by breast carcinomas. *J. Biol. Chem.*, **269**, 16766–16773.
- Nielsen,B.S. *et al.* (2001) Collagenase-3 expression in breast myofibroblasts as a molecular marker of transition of ductal carcinoma *in situ* lesions to invasive ductal carcinomas. *Cancer Res.*, **61**, 7091–7100.
- Johansson,N. *et al.* (1999) Collagenase-3 (MMP-13) is expressed by tumor cells in invasive vulvar squamous cell carcinomas. *Am. J. Pathol.*, **154**, 469–480.
- Airola,K. *et al.* (1997) Human collagenase-3 is expressed in malignant squamous epithelium of the skin. *J. Invest. Dermatol.*, **109**, 225–231.
- Airola,K. *et al.* (1999) Expression of collagenases-1 and -3 and their inhibitors TIMP-1 and -3 correlates with the level of invasion in malignant melanomas. *Br. J. Cancer*, **80**, 733–743.
- Pendas,A.M. *et al.* (2000) An overview of collagenase-3 expression in malignant tumors and analysis of its potential value as a target in antitumor therapies. *Clin. Chim. Acta*, **291**, 137–155.
- Luukkaa,M. *et al.* (2006) Association between high collagenase-3 expression levels and poor prognosis in patients with head and neck cancer. *Head Neck*, **28**, 225–234.
- Rizki,A. *et al.* (2008) A human breast cell model of preinvasive to invasive transition. *Cancer Res.*, **68**, 1378–1387.
- Uria,J.A. *et al.* (1997) Regulation of collagenase-3 expression in human breast carcinomas is mediated by stromal-epithelial cell interactions. *Cancer Res.*, **57**, 4882–4888.
- Wu,N. *et al.* (2003) Comparison of mouse matrix metalloproteinase 13 expression in free-electron laser and scalpel incisions during wound healing. *J. Invest. Dermatol.*, **121**, 926–932.
- Inada,M. *et al.* (2004) Critical roles for collagenase-3 (Mmp13) in development of growth plate cartilage and in endochondral ossification. *Proc. Natl Acad. Sci. USA*, **101**, 17192–17197.
- Stickens,D. *et al.* (2004) Altered endochondral bone development in matrix metalloproteinase 13-deficient mice. *Development*, **131**, 5883–5895.
- Madlener,M. *et al.* (1998) Matrix metalloproteinases (MMPs) and their physiological inhibitors (TIMPs) are differentially expressed during excisional skin wound repair. *Exp. Cell Res.*, **242**, 201–210.
- Hartenstein,B. *et al.* (2006) Epidermal development and wound healing in matrix metalloproteinase 13-deficient mice. *J. Invest. Dermatol.*, **126**, 486–496.
- Lafleur,M.A. *et al.* (2005) Upregulation of matrix metalloproteinases (MMPs) in breast cancer xenografts: a major induction of stromal MMP-13. *Int. J. Cancer*, **114**, 544–554.
- Nielsen,B.S. *et al.* (2008) Matrix metalloproteinase 13 is induced in fibroblasts in polyomavirus middle T antigen-driven mammary carcinoma without influencing tumor progression. *PLoS ONE*, **3**, e2959.
- Vosseler,S. *et al.* (2005) Angiogenesis inhibition by vascular endothelial growth factor receptor-2 blockade reduces stromal matrix metalloproteinase expression, normalizes stromal tissue, and reverts epithelial tumor phenotype in surface heterotransplants. *Cancer Res.*, **65**, 1294–1305.
- Vosseler,S. *et al.* (2009) Distinct progression-associated expression of tumor and stromal MMPs in HaCaT skin SCCs correlates with onset of invasion. *Int. J. Cancer*, **125**, 2296–2306.

37. Miller, D.W. *et al.* (2005) Rapid vessel regression, protease inhibition, and stromal normalization upon short-term vascular endothelial growth factor receptor 2 inhibition in skin carcinoma heterotransplants. *Am. J. Pathol.*, **167**, 1389–1403.
38. Fusenig, N.E. *et al.* (1983) Growth and differentiation characteristics of transformed keratinocytes from mouse and human skin *in vitro* and *in vivo*. *J. Invest. Dermatol.*, **81**, 168s–175s.
39. Fusenig, N.E. *et al.* (1978) Characteristics of chemically transformed mouse epidermal cells *in vitro* and *in vivo*. *Bull. Cancer*, **65**, 271–280.
40. Stacey, A. *et al.* (1997) Routine testing of cell cultures and their products for mycoplasma contamination. *Methods Mol. Biol.*, **75**, 305–311.
41. Todaro, G.J. *et al.* (1963) Quantitative studies of the growth of mouse embryo cells in culture and their development into established lines. *J. Cell Biol.*, **17**, 299–313.
42. Mueller, M.M. *et al.* (2004) Friends or foes—bipolar effects of the tumour stroma in cancer. *Nat. Rev. Cancer*, **4**, 839–849.
43. Obermueller, E. *et al.* (2004) Cooperative autocrine and paracrine functions of granulocyte colony-stimulating factor and granulocyte-macrophage colony-stimulating factor in the progression of skin carcinoma cells. *Cancer Res.*, **64**, 7801–7812.
44. Pfaffl, M.W. (2001) A new mathematical model for relative quantification in real-time RT-PCR. *Nucleic Acids Res.*, **29**, e45.
45. Cowell, S. *et al.* (1998) Induction of matrix metalloproteinase activation cascades based on membrane-type 1 matrix metalloproteinase: associated activation of gelatinase A, gelatinase B and collagenase 3. *Biochem. J.*, **331**(Pt 2), 453–458.
46. Overall, C.M. *et al.* (2002) Strategies for MMP inhibition in cancer: innovations for the post-trial era. *Nat. Rev. Cancer*, **2**, 657–672.
47. Bergers, G. *et al.* (2000) Matrix metalloproteinase-9 triggers the angiogenic switch during carcinogenesis. *Nat. Cell Biol.*, **2**, 737–744.
48. Zigrino, P. *et al.* (2009) Stromal expression of MMP-13 is required for melanoma invasion and metastasis. *J. Invest. Dermatol.*, **129**, 2686–2693.
49. Fallowfield, J.A. *et al.* (2007) Scar-associated macrophages are a major source of hepatic matrix metalloproteinase-13 and facilitate the resolution of murine hepatic fibrosis. *J. Immunol.*, **178**, 5288–5295.
50. Zijlstra, A. *et al.* (2004) Collagenolysis-dependent angiogenesis mediated by matrix metalloproteinase-13 (collagenase-3). *J. Biol. Chem.*, **279**, 27633–27645.
51. Toriseva, M.J. *et al.* (2007) Collagenase-3 (MMP-13) enhances remodeling of three-dimensional collagen and promotes survival of human skin fibroblasts. *J. Invest. Dermatol.*, **127**, 49–59.
52. Knauper, V. *et al.* (1997) The role of the C-terminal domain of human collagenase-3 (MMP-13) in the activation of procollagenase-3, substrate specificity, and tissue inhibitor of metalloproteinase interaction. *J. Biol. Chem.*, **272**, 7608–7616.
53. Licht, A.H. *et al.* (2006) JunB is required for endothelial cell morphogenesis by regulating core-binding factor beta. *J. Cell Biol.*, **175**, 981–991.
54. Goerges, A.L. *et al.* (2004) pH regulates vascular endothelial growth factor binding to fibronectin: a mechanism for control of extracellular matrix storage and release. *J. Biol. Chem.*, **279**, 2307–2315.

Received May 6, 2009; revised September 8, 2009; accepted October 10, 2009